μ-metal magnetic cavities for polarization and maintenance of polarization of ^{3}He gas

Earl Babcock, Zahir Salhi, Artem Feoktystov, Lester Barnsley, Jörg Voit, Kendal Bingöl, Simon Staringer, Stefan Mattauch, Alexander Ioffe

Jülich Centre for Neutron Science (JCNS) at Heinz Maier-Leibnitz Zentrum (MLZ),Forschungszentrum Jülich GmbH, 85747 Garching, Germany
Jülich Centre for Neutron Science (JCNS) and Peter Grünberg Institut (PGI), JARA-FIT Forschungszentrum Jülich GmbH, 52425 Jülich, Germany

E-mail: e.babcock@fz-juelich.de

Abstract. Low gradient magnetic holding fields are required for maintaining the polarization of polarized ^{3}He, as due to diffusion though gradients can cause relaxation much greater than relaxation of the gas storage container and the self-relaxation of the gas itself. For neutron scattering applications we often rely on μ-metal cavities to provide a degree of shielding from the many other sources of magnetic fields and gradient experienced on a typical neutron instrument. The JCNS utilizes two concepts for such cavities, one based on inexpensive plastic-bonded magnets to provide magnetic flux, and the other based on field coils wound on the sides of the μ-metal cavity. 2 different sized of permanent magnet cavities and three different geometries of coil-based cavities have been produced. Both types of boxes will be presented with magnetic design as well as mechanical construction details along with the achieved performance of the constructed devices.

1. Introduction

At the JCNS we use, or plan to use, polarized ^{3}He on a wide variety of instruments [1]. Where ever possible this polarization is to be done *in-situ* to reduce maintenance and to maximise the time averaged performance, especially for the case of long experiments lasting several days or weeks. Additionally to *in-situ* polarizers one also must often transport ^{3}He cells polarized in the laboratory to the neutron instrument and also for test experiments or temporary installations. All of these applications require a highly uniform magnetic field, providing where possible gradients on the order of 1×10^{-4} cm^{-1} for a typical ^{3}He cell with 1 bar pressure. One particular solution utilises magnetized rectangular μ-metal tunnels, these magnetic tunnels, colloquially referred to as "magic boxes" [2]. These cavities have a magnetic field transverse to the axis of the tunnel making them very suitable for beam applications and to help to fully decouple optical pumping access from the neutron path in the case of *in-situ* polarization. For the case of *in-situ* polarization we accomplish this with magic boxes magnetized by resistive field coils wound uniformly around their sides. For the transport and temporary/testing installations we have also developed magic boxes that use plastic bonded magnets for the magnetic flux source.

The coil based design has the largest homogenous volume over its cross section whereas the permanent magnet version has the added benefit that it doesn't require a power supply, both

versions have similar length constraints due to geometric requirements for magnetically isolating the ^{3}He cell from external field sources. For *in-situ* polarization applications three resistive coil cavities have been produced for different neutron polarization/scattering geometries, two of which deviate from a strait rectangular tunnel geometry to provide better magnetic shielding from sample environment/magnets, the larger magic boxes have essentially dipole-dipole limited relaxation times on beam and experience little influence from external magnetic fields on the ^{3}He [1]. Further two different permanent magnet versions based on a similar principle have been constructed, a 20 cm x 50 cm x 80 cm large box with a 4000 hour magnetic lifetime of ^{3}He gas at 1 bar pressure, and a smaller hand-transportable version that is 15 cm x 40 cm x 50 cm. The principles of design are general and could be applied to construct low magnetic gradient cavities at moderate magnetic fields (10-30 G) of nearly any rectangular-tunnel size which we will discuss fully in upcoming work. We note the full relaxation rate for ^{3}He in a magnetic field is given by

$$\Gamma_{He} = \frac{1}{T_1} = \frac{[He]}{800} + \frac{7000}{[\mathrm{He}]}\frac{\Delta B_x^2 + \Delta B_y^2}{B^2} + \frac{1}{T_{\mathrm{wall}}} \quad (1)$$

where in this coordinate system for our field geometries the direction of the field is $B_0 \simeq B_z$ and ΔB_x and ΔB_y are the orthogonal gradients, Γ_{He} is the total ^{3}He relaxation rate, which is the inverse of the cell lifetime T_1, and [He] in the ^{3}He pressure in bar. The first term on the left hand side is the dipole-dipole limit [3], the last term is the wall relaxation of a particular cell [5], and the middle term is the field gradient relation [4]. In this paper we will simply plot B_z so the expected ^{3}He relaxation cannot be directly inferred from the data, but it is a solid "visual" indication of low transverse gradients which are fully extracted from FEM calculations when designing a new magnetic configuration in order to estimate the expected volume averaged ^{3}He cell magnetic relaxation rate.

When possible we make our magic boxes long enough to shield the inner homogeneous volume from external field sources, and in this limit the geometry insures a fundamentally uniform and isolated field like that of long (shielded) solenoids. A diagram of an idealized coil-driven magic box sowing how we define the length L, width W and height H is shown in figure 1. Using FEM calculations one can determine the length Λ required to isolate the homogeneous region from external fields then a total box length of $2\Lambda + l$ will be required where l is the length of the homogenous region desired or the ^{3}He cell. For magic boxes whose cross-sections have aspect ratio, $a = W/H < 1$ the FEM calculations show $\Lambda \simeq W$ and for $a > 1$, Λ approaches a value of about $2W$.

2. Coil-generated flux magic boxes

We have made several versions of magic-boxes that have the field generated with coils. These consist of two basics types, shown in fig. 2. The one in the drawing on the right is a standard rectangular tunnel as discussed above which was produced for incident beam polarization of the thermal spectrum neutron beam for TOPAS [6]. The completed device has been recently used for user experiments on the POLI instrument [7, 8]. Originally we also constructed the MARIA polarization analysis system [9] with the same geometry at the TOPAS magic box, but with $W = 30$ cm [11]. While this magic box performed well in isolated conditions, the magnetic configuration and sample magnet of the MARIA instrument led us to produce the magic box shown in the drawing on the left. As will be discussed in this section, this MARIA magic box was rotated by 90 °, to make its field orthogonal to the sample field's magnet, and the fist set of yokes was rotated inward toward the neutron path by 45 ° resulting in the improved design that is shown. This particular design has also been duplicated, in the form of a magic box with 50% the size of the MARIA box for use on KWS1 [10]. This section will discuss the real world properties of magic boxes for specific installations as well as the reasons for these modifications to the MARIA analyzer magic box.

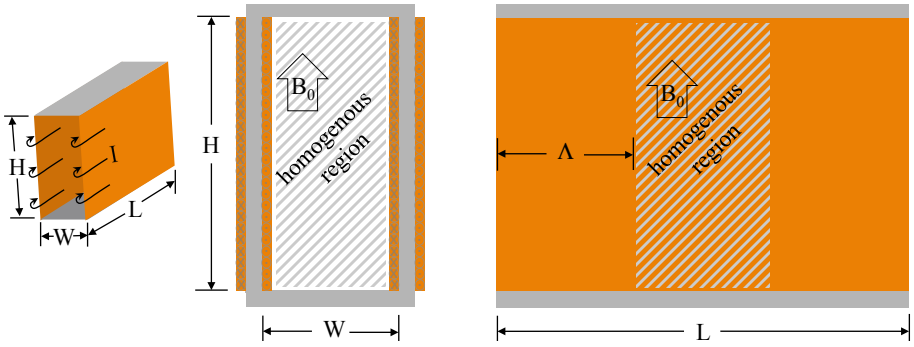

Figure 1. A diagram of an idealized magic box. The geometry is a perfect rectangular tunnel of μ-metal and the μ-metal has very high, and non-saturating permeability. The coils on either side (orange) are wrapped around the μ-metal and are perfectly uniform current sheets that extend from the bottom to top of the sides. The direction of the current, I in the current sheets in indicated with the arrows in the left hand side diagram.

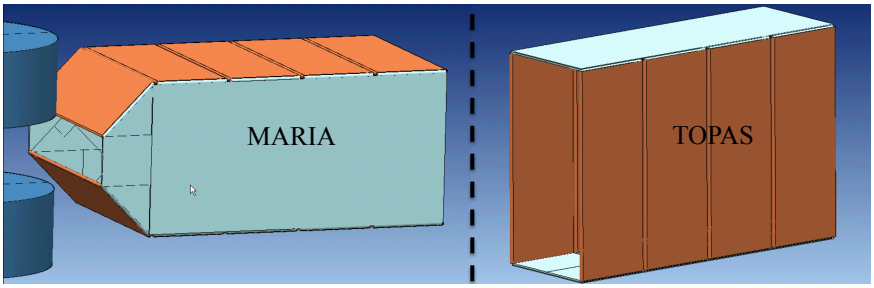

Figure 2. Drawings of two types of coil-driven magic boxes, the TOPAS style on the right is well suited to incident beam polarization, whereas the MARIA style on the left is well suited to wide angle scattered beam applications as a polarization analyzer.

Real world magic boxes obviously cannot fully conform to the ideal of perfectly sharp corners of perfect and non-saturating magnetic permeability, and ideal uniform current sheets, nor can they be constructed perfectly parallel. The real permeability curves which generally have saturation for 0.6 T/m for common μ-metal alloys, and the corners would either need to be welded, or bent with a radius to prevent air gaps which quickly spoil the uniform distribution of magnetic flux from the side "yoke" pieces to the top "pole" plates. Further the μ-metal itself must be sufficiently thick, such that the flux generated by the field coils stays sufficiently below saturation so that the permeability of the μ-metal retains its idealized properties of a high slope in the permeability, i.e. it continues to behave linearly with added magnetic flux. In practice we keep the calculated in the μ-metal below about 1/3 the value of the saturation in our calculations and this has produced good real-world performance for us. In the results of calculations for the TOPAS magic box shown in fig. 4 one immediately sees that the highest magnetization occurs in the middle of the side yoke plates which have the field coils on them. For example in a the magic box we have constructed for polarization on TOPAS [6, 8] the cross section of the box is 20 cm wide by 40 cm tall and we used 3 mm thick μ-metal with a turn density of 0.5 turn/mm at a current of 2 amps. In this case the magnetization of the μ metal is calculated to be 0.19 T, whereas for the 30 cm wide box used on MARIA [1] the μ-metal magnetization calculates to be 0.23 T. The thickness of the μ-metal helps to avoid saturation, however we often use 3 mm

thick μ-metal for other mechanical considerations also. In the limit where the permeability of the μ-metal is linear the magnetization in the yokes will approximately increase linearly with the width and the height of the magic box and also with current density. Conversely, the magnetization of the yokes decreases linearly with the thickness of the μ-metal. Thus higher magnetic fields, and larger cross section magic boxes can be constructed by appropriately scaling these parameters. Further, in practice we do not use a full 1 A mm^{-1} but rather 0.75 A mm^{-1}, resulting in a 30 kHz Larmour frequency for the ^{3}He atoms, which lowers the magnetization of the yokes correspondingly.

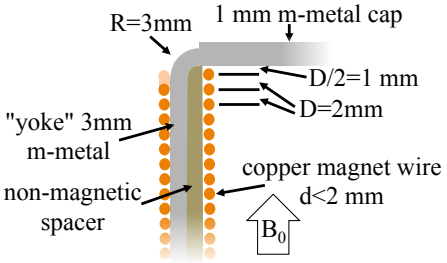

Figure 3. A diagram showing details of a real world device. The coils have windings parallel to the inside surface of the top and bottom pole plates and have a uniform and mirror-plane symmetry with respect to each. The windings return diagonally on the outside of the yokes and the coils are connected in series outside of the magic box. We use an inner radius of $R = t$ where t is the thickness of the μ-metal. In order to maintain the wire spacing and placement with respect to the top and bottom plates, a non-magnetic guide piece is machined with the wire locations and placed on the edges of the yokes and the wire is epoxied in place.

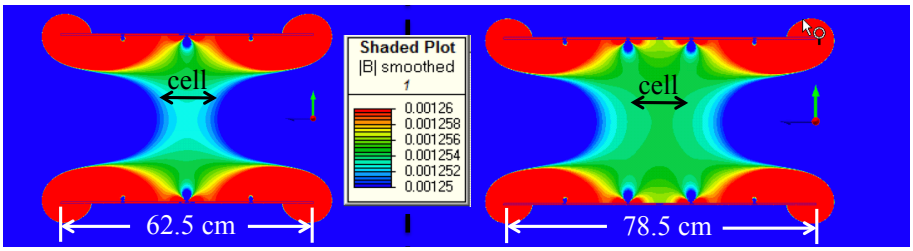

Figure 4. FEM calculations of the TOPAS magic box showing the longitudinal cross-section through the middle in two different lengths, 62 cm (middle) and 76.5 cm (right) where the field is vertical. One sees that using a measured curve for the μ-metal permeability one obtains a 0.19 T maximum magnetization in the yokes of this box at 1 A mm^{-1} current density, about 1/3 of saturation. Further we see that the shorter magic box, while not completely isolated from the external environment, does indeed provide good field homogeneity over the 15 cm length of the ^{3}He cell "Goldorack" used[13]. Each colour step is a 4×10^{-4} change in $\Delta B/B$.

For the next issue of the corners we have found that it is not important that the coil is tight to the the μ-metal plate, but rather that the windings are strait on the inside of the box, and are as uniform in spacing and symmetric with respect to the top and bottom of the μ-metal tunnel. A diagram of the corner configuration to do this is given in fig. 3. The gap between the the side plates on which the field coils are wound and the parallel surfaces of the top and bottom plates is simply filled with a nonmagnetic spacer material such as plastic or aluminium. The wires are then held at the proper spacing and position via. a half round edge piece which has v-groves machined in it at the positions of the center of each turn. In this way the wire position and spacing become independent of the wire diameter and variations therein and thus

any wire diameter less than the turn spacing can be used pending the balance of current values and resistance desired. For practical considerations due to the difficulty of guiding the wire strait from one edge of a μ-metal plate to the other, in practical devices we tend to use several shorter coil-plates, which we can consider like magnetic yokes, one after the other to build up to the desired total length. A small space on the order of 1.5 cm between the plates is required to have room to wind the coils around the plates, but this gap causes no problems because the gradients and penetration of external fields through them will only occur on a distance approximately equal to this gap. Since all our coil-driven magic boxes are constructed for online polarization, the additional space required for installation of an AFP solenoid-coil, furnace and laser optics ensures that the ^{3}He cell will never occupy a space this close to the gaps in the μ-metal yokes. The top and bottom plates which can be considered as pole-plates are assembled to be continuous so there is a flat and parallel surface between the top and bottom. the problem of air-gaps between them is solved by adding an extra thin μ-metal plate on the outside top and bottom of the box that is continuous for the whole length of the box.

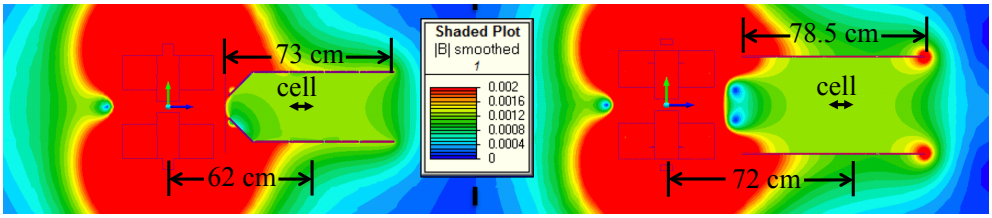

Figure 5. Results of FEM calculations of the new (left) and the old (right) MARIA magic boxes with the sample magnet turned on to a high field showing a slice though the axis. In each image the sample magnet is to the left and the magic box to the right. In the new MARIA magic box, the field of the sample magnet is vertical and the field of the magic box is orthogonal and out of the plane whereas in the old MARIA magic box, both fields are vertical and one can see the cause of the experimentally observed neutron depolarization in the scattered neutron beam. Not only does the new/improved magic box avoid these problems, but it also allow the ^{3}He cell to be placed about 10 cm closer to the sample position, increasing the angular coverage for the same size ^{3}He cell.

For the actual magic box for TOPAS the initial design was to follow our $2\Lambda + l$ rule which would have required a magic box about 75 cm long for good isolation from stray fields. However in the case of this device, since it is used in a location far away from the sample magnet, where the only stray fields will be from the fixes magnetic neutron guide fields at the exit to this polarizer we constructed it 62.5 cm long as shown in the left of fig. 4. Additionally the thermal energies used on TOPAS required use of a ^{3}He cell with a 3 bar bar pressure to obtain an acceptable polarizing efficiency which from equation 1 will also be less sensitive to field gradients than the typical $\simeq$ 1 bar cells used for cold neutron beams [12].

As an improvement on this initial rectangular tunnel design, we have found that one can decrease the effective opening width of such boxes by angling the fist set of plates inward toward the magic box axis. This was discovered in an initial installation of the MARIA polarized ^{3}He analyzer system which had the magnetic field in the box vertical, i.e. parallel to the normal sample fields used on this instrument. Fig. 5 shows a FEM calculation with a model of the 1.2 T (with 5 cm gap and 2.2 T with reduced 2 cm gap) sample magnet included. Even though this magnet has a yoke and in air does not produce large stray fields over 10's of gauss 10 cm away from the perimeter, we see that the addition of a high permeability object near it, in this case our magic box, causes coupling of the return field into the magic box. While the ^{3}He lifetime was not yet severely affected, as can be seen in fig. 5 low field areas are created inside the magic box

above and below the center which caused depolarization effects in our scattered neutron beam. To solve this problem, the first step was to rotate the magnetic field axis of the magic box by 90 degrees which eliminated the problem of the return fields of the sample magnet subtracting from the field of the magic box and the field overlaps are sufficient for fully adiabatic rotation of the neutron polarization. Then as a further improvement, we rotated the first yoke piece of the five used on either side, toward the center by 45 degrees decreasing the effective opening of this magic box in the direction towards the sample magnet. As can be seen comparing this new configuration to the old one in fig. 5 these modifications allowed us to move our 12 cm diameter ^{3}He cell approximately 10 cm closer to the sample position, while solving both the problem of magnetic coupling and neutron depolarization of the scattered beam.

The magnetic lifetime for this MARIA box is very good, as it obtains a total lifetime of 380 hours for the cell "Idafix" used [13], which within errors is the same as the value obtained for this cell in "ideal" laboratory conditions and therefore produces a nearly ideal field. The smaller magic box produced for KWS1 produces a 180 hour magnetic lifetime. The field of this compact magic box is not as uniform as the larger boxes simply because its small 50% size increases the ^{3}He relaxation by a factor of four from eq. 1 and because of the greater mechanical precision required for such a small cavity. However its performance is sufficient for *in-situ* polarization which can easily obtain ^{3}He polarization rates of under 10 hours. The box for TOPAS achieved a 200 hour total T_1 (using a the 3 bar cell "Goldorack" with a 220 hour T_{cell}[13]) or a 700 hour magnetic lifetime for 1 bar and has produced excellent ^{3}He *in-situ*polarization results [8].

3. Permanent magnet magic boxes

Permanent magnet magic boxes rely on similar principles, but now the magnetic flux in the μ-metal side pieces will be provided by (uniform) permanent magnet strips at discrete locations. We use a particular product from IBS Magnets called Betaflex® which is a flexible plastic-bonded magnet that provides a 0.245 T remanence [14]. The use of such a magnet is very important because as it is made of a uniform distribution of hard magnetic particles in plastic it produces a magnetization independent of the width to length ratio and in a direction of ones choice.The remanence value is also important, most magnets such as NbFeB, AlNiCo, or even ferrite have higher saturation magnetizations than can be transported by the μ-metal without saturating it. At 0.245 T, the flux provided by these betaflex magnet strips is still far enough below the 0.6 T μ-metal saturation, that for magnet strip widths equal to the thickness of the μ-metal, or even a bit wider, the μ-metal can not be saturated by these magnets and thus stays in the approximately linear and isotropic regime. This is of advantage over device such as those presented in [2] because there is no need for additional iron components, special construction/tolerances or magnet selection in order to guide the magnetic flux along the μ-metal of the side plates of the magic box while fundamentally avoiding saturation of the μ-metal.

To first order as we illustrate in fig. 6 the Betaflex ® magnet strips would be placed at mirror-plane symmetric intervals from the μ-metal top and bottom plates in order to achieve a uniform field configuration. An arbitrary number of strips in principle could be used, however for simplicity of construction we use two. Since the field is un-uniform near the magnets, one must increase the width of the box a bit over two times the magnet spacing plus the desired width of the homogenous region. With this condition for the width added to the requirements for the tunnel length from section one we arrive at a baseline for the design of a permanent magnet magic box. Both effects can be seen in fig. 7 which shows the FEM calculations for our two sizes of permanent magnet magic boxes.

^{3}He In practice, real world constraints such as rounded corners and a real height of the magnet strips causes the optimal configuration to vary slightly from the ideal mirror-plane location of the magnetic strips. This precise location is thus determined with FEM calculations where we start with the magnet strips in the ideal locations, and move them symmetrically towards or

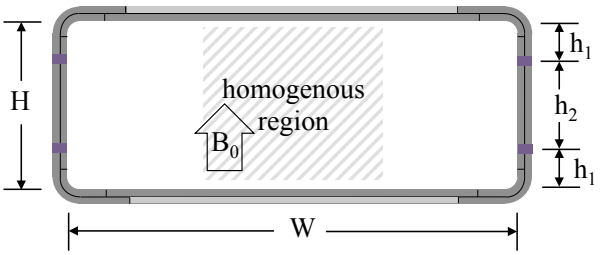

Figure 6. A schematic drawing of our permanent magnet magic boxes. The Betaflex ® [14] magnetic rubber strips are indicated as purple and their magnetization is downward. The radius of the corners used is 1 cm and the box is made of two layers of 1.5 mm μ-metal held together with non-magnetic screws through it to an external frame. The sides with the permanent magnet strips are clamped together with non-magnetic plates made of PVC bolted through the side pieces, again with non-magnetic bolts. The upper and lower plates drawn at light grey are optional and not used in constructed magic boxes to reduce weight.

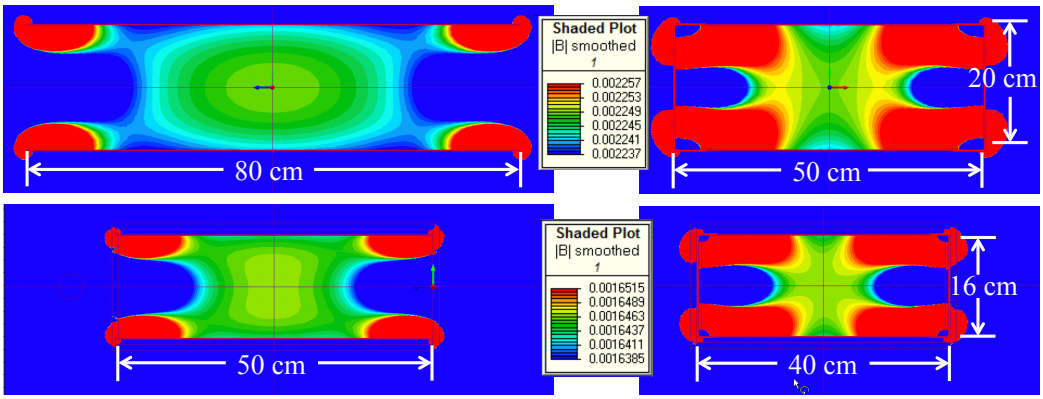

Figure 7. FEM calculations of our two permanent magnet magic boxes, the large version on top and the smaller version below. Left is a longitudinal cross-section and right is an on-axis slice both through the center. One can easily see how the end-effects affect the total length and homogeneous region, and how the permanent magnet strips affect the required width. Each colour step is a 5×10^{-4} change in $\Delta B/B$

away from the box center-line until the optimal location with the minimum volume averaged magnetic field gradient over the desired area is achieved. We have constructed two sizes of permanent magnet magic boxes, one is calculated for $H = 20$ cm by $W = 50$ cm and $L = 80$ cm, the other is $H = 16$ cm by $W = 40$ cm and $L = 40$ cm. After this numerical optimization, the midpoint of the 0.5 cm high magnet strips was found to be 5.75 cm away from the center-line of the magic box was determined to be the best for the larger box, and 5.25 cm away from the center line for the smaller box. FEM calulations of these two magic boxes are shown in fig. 7.

For the actual construction we use two layers of 1.5 mm thick μ-metal stacked together and PVC plastic plates to hold the side pieces and Betaflex® magnet strips in place. The 1.5 mm thick μ-metal is only doubled on the sides and corners and the top and bottom pole plates are just a single layer to reduce weight. The whole magic box is then mounted in either a PVC plastic frame for the smaller one or an aluminium profile frame for the larger version. These

boxes are very resilient to construction parameters to achieve a homogeneity required for the temporary storage and transport of polarized ^{3}He gas. The larger version gave a measured ^{3}He magnetic lifetime in excess of 5900 hours by measuring the reduction in T_1 of a 200 cm^3 ^{3}He cell called "J1" which has 1 bar ^{3}He and a $T_1 = 690$ in ideal conditions. The smaller version by chance was constructed with an $H = 15$ cm and the magnet strips placed at 2.75 cm away from the box center line and this one gives a ^{3}He magnetic relation time of 1000 hours measured in the same way as the large box, which is very acceptable for transport applications. In principle the as calculated box could have on the order of a 2x more uniform magnetic field (leading to a 4x longer magnetic lifetime for polarized ^{3}He) over a larger area in the center of the box, but considering its relaxation rate is still a slower than the intrinsic decay rate in ideal field conditions of typical ^{3}He NSF cells it is more than sufficient as constructed. An additional copy of the large box was also constructed and gave comparable results to the first one.

4. conclusions

We present several geometries of "magic boxes" that obtain high performance for practical applications utilizing polarized ^{3}He. Several coil-driven magic boxes have been made with magnetic lifetimes at one bar of ^{3}He pressure of 180 hours, 700 hours and dipole-limited for the KWS1, TOPAS and MARIA systems respectively [10, 8, 9]. Further we have applied the same principle to produce permanent magnet magic boxes of two different sizes, the larger with an achieved magnetic lifetime of 5900 hours and the smaller with 1000 hours again for one bar ^{3}He pressure. The coil-driven magic boxes are especially useful for *in-situ* optical pumping with SEOP and instrumentation, whereas the permanent magnet boxes are ideal for transportable devices, and passive or off-line polarized applications. Further we expect these devices are of utility to other fields where convenient low-gradient magnetic field geometries in compact and shielded formats are required. We would like to thank SOME PEOPLE, blah blah blah.

References

[1] E Babcock, Z Salhi, T Theisselmann, D Starostin, J Schmeissner, A Feoktystov, S Mattauch, P Pistel, A Radulescu, A Ioffe, J. of Physics Conf. Series **711** (1) (2016) 012008.
[2] A K Petoukhov, V Guillard, K H Andersen, E Bourgeat-Lami, R Chung, H Humblot, D Jullien, E Lelievre-Berna, T Soldner, F Tasset, M Thomas, Nuclear Instruments and Methods in Physics Research A **560** (2006) 480-484.
[3] N R Newbury, A S Barton, G D Cates, et al., Phys. Rev. A **48** (1993) 4411-20.
[4] G D Cates, S R Schaefer, W Happer, Phys. Rev. A **37** (1988) 2877-85.
[5] T R Gentile, P J Nacher, B Saam, T G Walker, Review of Modern Physics **89**(4) (2017) 045004.
[6] J Voigt, H Soltner, E Babcock, R J Aldus, Z Salhi, R R Gainov, T Brückel, EPJ Web of Conferences **83** (2015) 03016.
[7] Jülich Centre for Neutron Science am MLZ, *POLI: Polarised hot neutron diffractometer*, J of large-scale research facilities, 1, A16 (2015).
[8] Z Salhi, E Babcock, P Pistel, K Bussmann, H Kämmerling, V Ossovyi, H Deng, V Hutanu, S Masalovich, J Voigt, A Ioffe, this issue.
[9] S Mattauch, A Koutsioubas, U Rücker, D Korolkov, et. al., J of App Crystallography **51**(3) (2018) DOI: 10.1107/S1600576718006994.
[10] A V Feoktystov, H Frielinghaus, Z Di, S Jaksch, et. al., J of Appl Crystallography **48** (1) (2015) 61-70.
[11] E Babcock, S Mattauch, A Ioffe, Nuclear Instruments and Methods in Physics Research Section A: Accelerators Spectrometers Detectors and Associated Equipment **625** (2010) 43-46.
[12] Z Salhi, E Babcock, R Gainov, K Bussmann, H Kämmerling, P Pistel, M Russina, A Ioffe, J of Phys: Conference Series **711** (2016) 012013.
[13] Z Salhi, E Babcock, P Pistel, A Ioffe, J of Phys: Conference Series **528** (1) (2014) 012015.
[14] IBS Magnet, Kurfürstenstrae 92, D-12105 Berlin, https://ibsmagnet.com/products/dauermagnete/betaflex.php.